Small-Scale Study of Siberian Biomass Burning: II. Smoke Hygroscopicity

Olga B. Popovicheva[1]*, Natalia M. Persiantseva[1], Mikhail A. Timofeev[1], Natalia K. Shonija[2], Valerii S. Kozlov[3]

[1] *Skobeltsyn Institute of Nuclear Physics, Lomonosov Moscow State University, Leninskie Gory 1, 119991, Moscow, Russia*
[2] *Chemical Department, Lomonosov Moscow State University, Leninskie Gory 1, 119991, Moscow, Russia*
[3] *Institute of Atmospheric Optics, SB RAS, Zuev sq.1, 634021, Tomsk, Russia*

ABSTRACT

A lack of understanding about the impact of Siberian wildfire emissions on the environment necessitates the characterization of biomass burning aerosol hygroscopicity. Flaming fires of typical Siberian biomass (pine and debris) were simulated during small-scale combustion experiments in a Large Aerosol Chamber (LAC). Analyses of individual particles with respect to morphology and elemental composition allows the separation of freshly-produced smoke into five fractions with the elemental carbon, chain soot agglomerates, irregular internally mixed soot, and distinct irregular minerals of fly ash containing S, Ca, Al, and Si. Aging in a dark chamber leads to an appearance of the fraction with inorganic inclusions such as KCl and $CaCl_2$. Categorization of fresh-emitted and aged particles on hydrophobic, hydrophilic, and hygroscopic ones is performed. The criteria for categorization are extended from fossil fuel high-temperature combustion, based on a concept of water uptake by soot particles and utilization of a number of reference soots with known oxygen content and mixtures with sulfates and other inorganic salts. We show how the hydration properties of emitted smoke particles and inorganic inclusions can increase the initial level of smoke hygroscopicity.

Keywords: Biomass burning; Siberian wildfires; Smoke aerosol; Elemental composition; Fractionation; Water absorption; Hygroscopicity.

INTRODUCTION

Emission from combustion is known to be a major contributor to the global budget of ambient particulate matter (PM) and black carbon (BC), impacting air quality, incoming radiation, and increasing health hazards (Mieville *et al.*, 2010; van der Werf *et al.*, 2010). Biomass burning (BB) aerosols have gradually received wide attention owing to their importance in regards to BC impacts on the environment and the cloud radiation properties due to the aerosol indirect effect in form of increasing the concentration of cloud droplets by serving as cloud condensation (CCN) and ice nuclei (IN) (Ito and Penner, 2005; Popovicheva *et al.*, 2010).

Wildfires serve as a large source of CCN with a wide range of hygroscopicity and can be a source of heterogeneous ice nuclei (IN) with the number concentration of regional importance (Pratt *et al.*, 2011). Siberian wildfires are found to be a major source of climate-relevant species emitted at northern latitudes (Lavoué *et al.*, 2000). BB smoke in Siberia is a major contributor to the Arctic pollution (Paris *et al.*,

2009; Warneke *et al.*, 2010). Many studies show that emissions from forest fires not only constitute the local pollution but are also transport away from sources and have the potential to affect global atmospheric chemistry and cloudiness (Treffeisen *et al.*, 2007), while the assessment of Siberian BB emissions and their potential attribution to hygroscopicity effects is very limited.

The most general and useful concept of combustion aerosol is that it is a mixture of elemental carbon (EC), condensed hydrocarbons or organic carbon (OC), and water-soluble material, such as sulfur compounds in fossil fuel residuals or potassium and chloride in BB smoke. Analysis of water interaction with soot, being a product of high-temperature combustion of hydrocarbons, significantly improves the link between soot physico-chemistry and CCN formation (Koehler, 2009; Yun *et al.*, 2013). It has been shown that EC may be a constituent of hydrophobic particles, as oxygen-containing functionalities of organic carbon provide hydrophilic surfaces while the presence of water-soluble compounds leads to soot hygroscopicity and CCN activity (Popovicheva *et al.*, 2008a).

Many water-soluble compounds occur in BB smoke (Reid *et al.*, 2005), although soot does not seem to be a likely a candidate for containing significant amounts of such material. Potassium salts are commonly observed in

---

biomass smoke (e.g., Posfai *et al.*, 2003; Semeniuk *et al.*, 2007) and potassium and chloride are the most abundant ions in most burn emissions. It was concluded that carbonaceous particles with inorganic inclusions are likely responsible for the high cloud-nucleating potential of biomass smoke (Andreae and Rosenfeld, 2008).

Two mechanisms of water/soot interaction have been proposed: bulk dissolution into water-soluble coverage (hygroscopic soot) and the water molecule adsorption onto surface oxygen-containing functionalities (non-hygroscopic soot) (Popovicheva *et al.*, 2008b). The formation of a water film extended over the surface separates hydrophobic from hydrophilic soot. Simulations of fossil fuel combustion particles by deposition of various compounds identified in original transport emissions on laboratory-made soots proved the change of the mechanism of water/soot interaction from adsorption for hydrophobic soots to the dissolution into the water-soluble coverage of hygroscopic soots (Popovicheva *et al.*, 2009). Based on water uptake by EC, using soot covered by monolayers of sulfates, the transformation of soot hydration properties from hydrophobic, through hydrophilic, to hygroscopic ones was demonstrated (Popovicheva *et al.*, 2011).

A number of approaches were proposed to differentiate combustion particles with respect to their ability to take up water at the microscopic level. Okada and Hitzenberger (2001) separated combustion-derived PM into water-insoluble and hygroscopic particles with and without water-soluble inclusions. The separation into C-O, C-O-S, and Me-C-O fractions containing the chain soot agglomerates, irregular sulfur-internally mixed soot, and particles of insoluble impurities of mineral morphology, respectively, has allowed categorizing the transport engine-generated particles as hydrophobic, hydrophilic, and hygroscopic on the basis of concept of quantification of water uptake by soot (Kireeva *et al.*, 2009). Fractionation analysis of modern internal combustion engine emissions showed that the operation conditions under higher combustion air ratios lead to bigger concentrations of oxygen which are mostly responsible for hygroscopicity of emitted soot (Popovicheva *et al.*, 2015a). However, biomass burning aerosols still remain not addressed by this concept, because carbonaceous particles with inorganic inclusions were not including in the fractionation approach.

Various small-scale BB studies have been conducted in combustion chambers for characterization of morphology, composition, and hygroscopicity of smoke aerosols from biomass under controlled conditions (Petters *et al.*, 2009; Carrico *et al.*, 2010; Chakrabarty *et al.*, 2010; Li *et al.*, 2015). This approach allows to reduce uncertainties in wildfire studies, resulting from a mixture of fuels, impact of soil, wind, and unpredictable combustion phase. Hand *et al.* (2010) demonstrated a significant range in the hygroscopic properties of freshly-produced smoke from flaming and smoldering occurring simultaneously. They assumed that only inorganic salts take up water and organic particles are completely non-hygroscopic during growth of smoke particles in humid environments.

Optical and microphysical properties of aerosols from small-scale fires of Siberian biomass were investigated in a Large Aerosol Chamber (LAC) of the IAO, Tomsk (Rakhimov *et al.*, 2012). Individual particle analysis in terms of smoke morphology and elemental composition revealed a strong dependence on combustion temperature, i.e., a dominant abundance of soot agglomerates versus roughly spherical organic particles in the flaming and smoldering phase, respectively (Popovicheva *et al.*, 2015b). Cluster analysis separated pine wood and debris particles from flaming fires into major characteristic groups where Group Soot accounted for around 90% of total particle number. Small quantities of elemental constituents in biomass produced internally/externally mixed fly ash in Group Ca-, Si-, and Fe-rich of significantly less abundance. However, fly ash particles may produce those inorganic inclusions which are likely responsible for the high cloud-nucleating potential of biomass smoke. Moreover, during smoke aging in a chamber volatile inorganic compounds were found to condense and subsequently enlarging fly ash groups.

This paper investigates Siberian biomass burning by in-depth characterization of individual particle composition in relation to their hygroscopicity. The approach of fractionation analysis developed for fossil fuel – produced soots is applied to Siberian pine and debris smoke from flaming fires. Quantification of water absorption is extended for carbonaceous particles with inorganic inclusions by laboratory observations of water uptake on mixtures of inorganic salts with soot. This study provides further understanding of mechanisms and compounds responsible for water uptake by biomass smoke, including the categorization of hydrophobic/hydrophilic and hygroscopic particles in flaming emissions at microscopic level.

EXPERIMENTAL

Small-Scale Chamber Burns

Small-scale fires were performed in a Large Aerosol Chamber (LAC) with a total volume of 1800 m^3 under controlled combustion conditions. Experiments are described in detail in part I of the LAC study (Popovicheva *et al.*, 2015b). Briefly, high-temperature combustion was conducted in an oven centered in the LAC at temperatures ~700°C, simulating open fires in the flaming phase. The fuels used were dry biomass species from closed-canopy coniferous forest, scots pine wood and forest debris (mixture of pine needles, branches and cones). The smoke from each burn was allowed to fill the chamber and remain there for a period of 48 h in order to study the compositional smoke evolution over time without sunlight.

Polar spectronephelometery was used for PM measurement, as described in Rakhimov *et al.* (2014). After ignition the aerosol PM mass concentration was continuously rising and approached the maximum level typically in 2 hours, when smoke was dispersed and had filled the chamber homogeneously. At this time the sampling of fire-emitted particles was commenced; the smoke particles collected at this moment are term "fresh". To evaluate the time evolution, smoke was able to stay in a LAC during one-two days more, with continuous decreasing the PM mass concentration. That

one which we collected in 48 hours was called as "aged". The impactor with an aerodynamic cutoff diameter of 1.08 μm was utilized to collect particles on metal substrates (Cu foil) behind PM_{10} and $PM_{2.5}$ size-selective inlets. Several (3–6) replicate burns for each fuel were performed to investigate the burn-to-burn variability of the combustion process.

Chemical and Physical Analyses

Experimental characterization of BB aerosols focused on morphology and composition of individual particles for each biomass species. The smoke samples collected on Teflon filters were examined using a LEO 1430-vp (Karl Zeiss) field emission scanning electron microscope (SEM) with a spatial resolution of 7 nm, equipped with an Oxford energy dispersive detector INCA. Energy dispersive X-ray (EDX) spectra for Z elements ($Z \geq 5$) were recorded in SEM image mode and the measured X-ray intensity was quantified for the elemental weight percent with an accuracy of 0.3 wt%. Samples were studied in the high vacuum mode at 10 kV acceleration voltage and a beam current of 1 nA. Approximately 500–1000 individual particles with a diameter from 0.1 up to 2.5 μm and to 10 μm were measured in $PM_{2.5}$ and PM_{10} samples, respectively. This number is sufficient for obtaining a representative overview of individual elements and groups in each sample (Liu *et al.*, 2000; Chakrabarty *et al.*, 2006; Popovicheva *et al.*, 2014b). Data will be presented here as an average over three repeated burns for each combustion case. Since highly irregular and agglomerated shapes of particles prevent determination of the size distribution from SEM images, only averaged sizes of primary particles in chain agglomerates were estimated using their projected area equivalent diameters.

Previously, we used graphitized soot (GTS) as a basic EC soot substrate representing hydrophobic particles because of its well-characterized composition free from any impurities and perfect graphitic structure (Popovicheva *et al.*, 2009). Other reference soots have been produced by combustion of diesel fuel in a laboratory burner (DFF soot; Kireeva *et al.*, 2009), and gaseous propane/butane fuel in a gas turbine engine combustor (PBS soot; Popovicheva *et al.*, 2003). These soots are composed from agglomerates of roughly spherical primary particles with sizes between 20 and 50 nm, containing almost only C and O with a negligible water-soluble fraction. The proportion of particles with O/C ratios up to 7% and 12% was found by EDX in DFF and PBS soots, respectively. They were used in fractionation analyses of fossil fuel-generated soot produced by transport (diesel and aircraft) engines (Kireeva *et al.*, 2009).

In this study we used GTS, DFF, and PBS soots as references for flaming fire-generated smoke, assuming the mechanism of the particle formation during high-temperature combustion is similar regardless of fuel type. Water uptake *a* (mmol g^{-1}) was measured by a gravimetrical method, described elsewhere (Popovicheva *et al.*, 2009). To obtain the absolute adsorption isotherms for comparative analyses, we recalculated the *a* value from the amount of water monolayers (ML) assuming the measured surface area, S (m^2 g^{-1}), for a given soot. The number of monolayers was estimated as ≈ a·60/S assuming the cross-section area of a

water molecule to be 0.105 nm^2. To simulate the presence of sulfates, reference soot was used as the substrate and deposition of sulfuric acid from aqueous solutions on its surface was performed with coverage up to 15 wt% (Popovicheva *et al.*, 2011). Water uptake on soot mixed with sulfuric acid was quantified in dependence on wt% of H_2SO_4.

To simulate for water uptake by soot mixed with insoluble inclusions in this study we produced the mixtures of GTS soot with a given amount of aqueous solutions of KCl and $CaCl_2$ to get samples containing from 1 to 10 wt% of K and Ca. Because K and Ca can appear in different particles at various weight percentages, also in some particles independently, we prepared these mixtures separately.

After drying at 150°C, water uptake on simulated soot particles was measured by a similar way to that described above and quantified in dependence on wt% of insoluble inclusions.

RESULTS AND DISCUSSION

Fractionation with Respect to Morphology and Composition

Siberian biomass smoke particles sampled in the flaming phase show both chain aggregate and crystalline morphology. The major type of particles in pine and debris flaming emissions is soot, distinguished by agglomerates of ultrafine primary particles containing from a few up to hundreds of spheres (Fig. 1.1,2). The size distribution of primary particles is estimated for fresh pine smoke using the projected area equivalent diameters (Fig. 2). The mean diameter of 90 ± 30 nm was obtained from 200 particles.

EDX analysis of smoke from flaming fires shows the elements C, O, Ca, Al, Si, S, Cl, K, Fe, Ti, P, Na, Mg, and N at various weight concentrations. Nearly every particle in pine and debris smoke was found to be carbonaceous, i.e., its major elements are C and O. The weight percent of trace elements in $PM_{2.5}$ smoke particles is presented in Fig. 3, indicating O, Ca, S, Si and O, as well as Si, Al, Ca as the most significant elements in particles produced during pine and debris combustion, respectively. There is no significant difference between the composition of $PM_{2.5}$ and PM_{10} smoke, probably due to the concentration of coarse smoke particles being low. Therefore, from here we report only $PM_{2.5}$ data. Time evolution of flaming smoke in the chamber led to a prominent increase of the weight percent of K, Cl, and S in particles, by factor of 5.7, 6, and 12, respectively (Fig. 3).

For the following hygroscopicity analyses, the individual particles are allocated into six fractions with respect to their elemental composition and morphology. The naming of the fractions and criteria is presented in Table 1. Table 2 shows the averaged composition of particle fractions in fresh and aged pine and fresh debris $PM_{2.5}$ smoke produced in flaming fires. The accuracy of the fraction separation is estimated around 1% associated with the presence of mixed particles composed from many elements.

Percentages of particles in fresh pine and debris smoke in each fraction are shown in Fig. 4. Relative abundances of 19.2% and 18.7% of particles in pine and debris smoke,
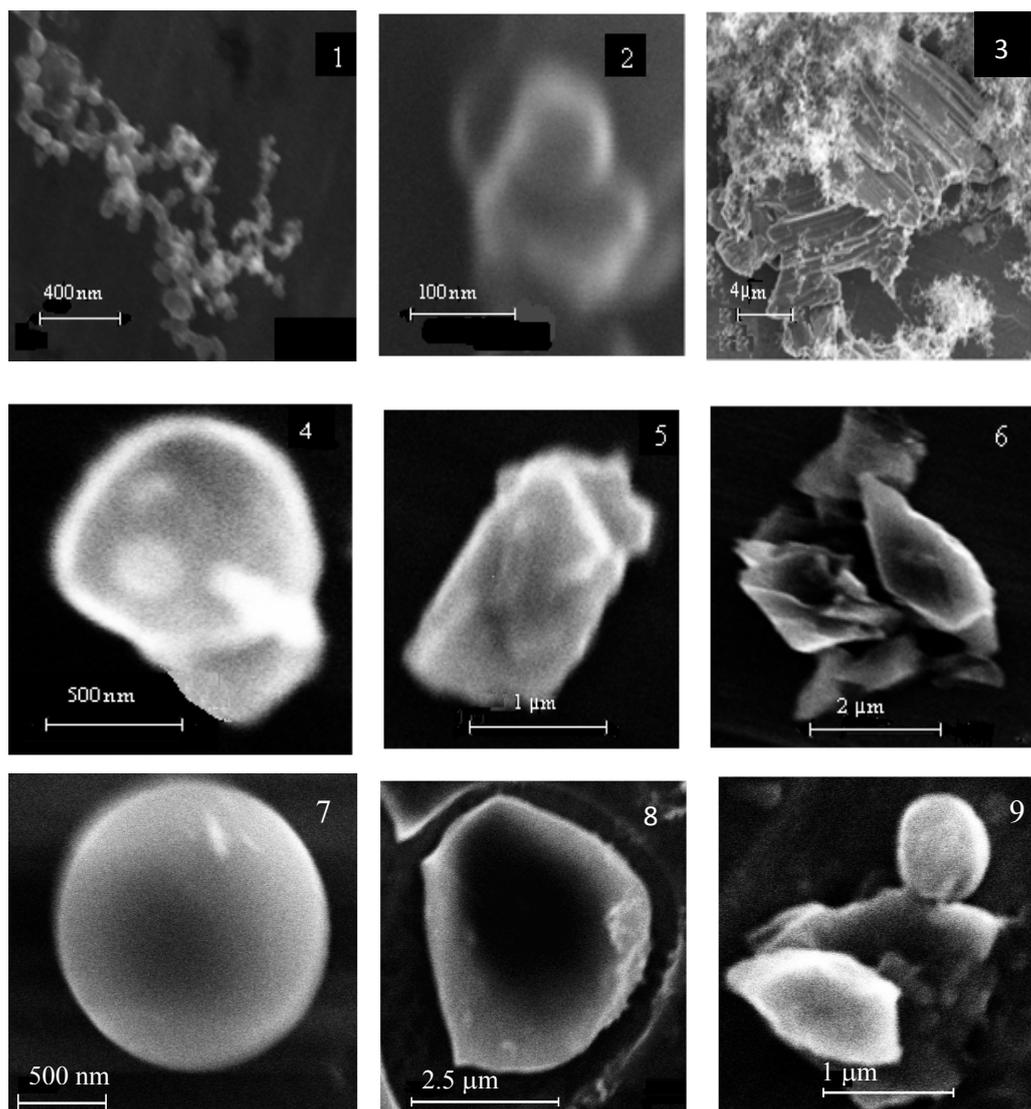
Fig. 1. Morphology of smoke particles from pine and debris flaming fires: in C-O fraction 1) soot agglomerates and 2) soot primary particles, 3) graphitic structure of EC, 4) particle with high organic content; in C-O-S fraction 5) irregular shaped sulfate particle; in C-O-Ca fraction 6) CaO/CaCO$_3$; in C-O-Al-Si fraction 7) Fe-aluminosilicate; in C-O-K-Cl fraction 8) KCl and 9) CaCl$_2$/CaSO$_4$.

respectively, are found containing only C; they are associated with EC and typically demonstrate soot morphology. Randomly we observed the perfect graphitic structures in the biggest particles of PM$_{10}$ smoke, as shown in Fig. 1.3. 67.7% and 70% of particles in pine and debris smoke, respectively, belong to the C-O fraction, since they consist entirely of carbon and oxygen, typically demonstrating soot morphology (Fig. 1.1,2). However, some of these particles appeared with compact morphology of fused particles instead of fractal shape (Fig. 1.4), as was observed in smoke emissions from flaming burns of other biomass species (Popovicheva *et al.*, 2014a). These particles probably contain OC with relative abundances in total carbon as high as 32% and 37% in pine and debris smoke, respectively (Popovicheva *et al.*, 2015b).

Percentages of particles containing sulfur at the largest concentrations after C and O in the C-O-S fraction in pine smoke were found to be small (3.8%), well in accordance with low fractions (~0.8%) of SO$_4^{2-}$ ions found in PM$_{2.5}$. Sulfates may be condensed on soot particles forming internally mixed soot and do not change soot morphology, as shown in Popovicheva *et al.* (2015b). They may also form irregular-shaped particles of salts (Fig. 1.5). No C-O-S particles were detected in fresh debris smoke with the given accuracy of our method.

Fractions of 5.7% and 3.4% of particles in pine and debris smoke are dominated by Ca after C and O in the C-O-Ca fraction. Calcium comprises on average 20 and 7 wt% in pine and debris smoke, respectively. These particles were observed with typical mineral angular shapes (Fig. 1.6), probably composed of calcium oxide (CaO) and/or carbonates (CaCO$_3$). Finally, 3.6% and 7% of all particles were comprised by the C-O-Al-Si fraction with dominance of Si and Al after C and O, and with minor content of K, Ca, Fe,
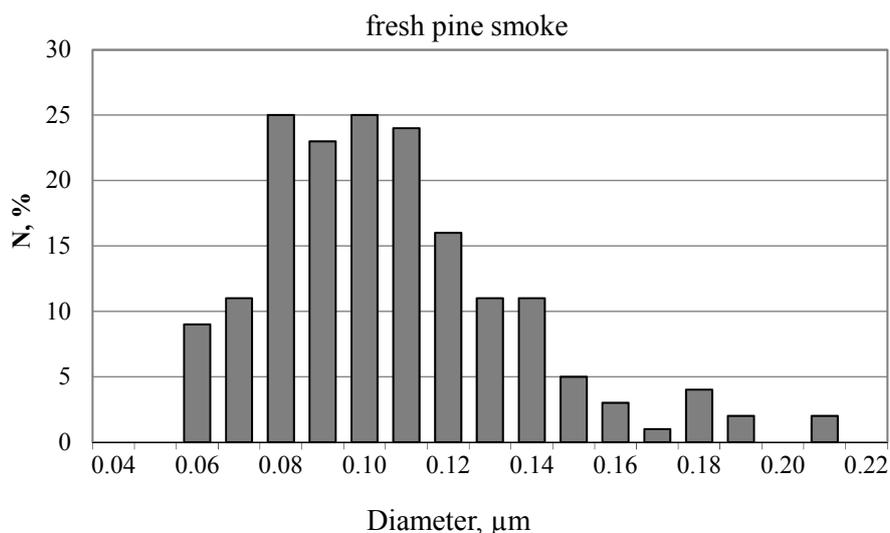
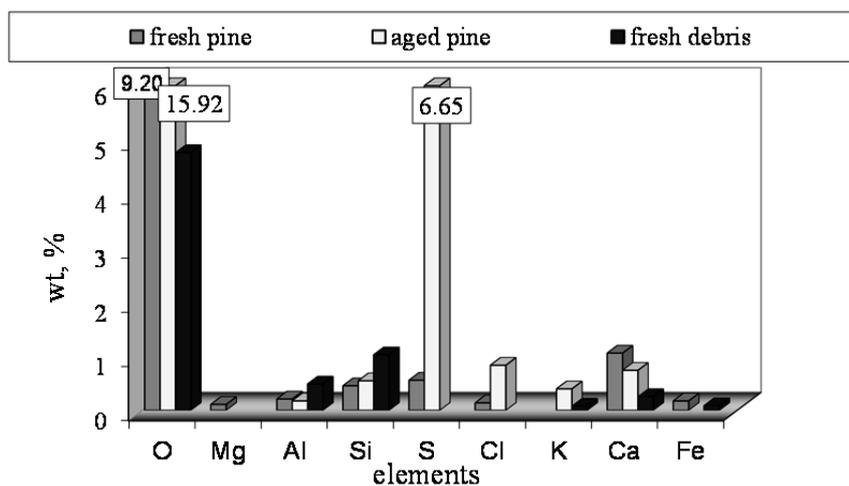**Fig. 2.** Size distribution of primary soot particles of fresh pine smoke.

Fig. 3. Weight percent of elements in fresh and aged pine, and in fresh debris smoke.

Table 1. Criteria for particle fractionation in pine and debris smoke produced in flaming fires.

Fraction	Elements	Morphology
C	C	chain agglomerates, minor graphitized structures
C-O	C and O, others ≤ 2%	chain agglomerates of spherical particles, compact morphology
C-O-S	C, O and S, minor Cl, K, Ca, Fe < 4%	internally mixed soot, irregular shapes
C-O-Ca	C, O and Ca, minor Mg < 2%	different angular shapes
C-O-Al-Si	C,O, Al and Si, minor K, Ca, Fe, Ni, Mg	variable irregular shapes
C-O-K-Cl	C,O, K, Cl, minor S, Ca	irregular shapes

Table 2. Averaged composition of particle ($PM_{2.5}$) fractions in fresh and aged pine and fresh debris smoke produced in flaming fires.

Fraction	Fresh pine	Aged pine	Fresh debris
C	C_{100}[1]	C_{100}	C_{100}
C-O	$C_{91}O_9$	$C_{86}O_{13}$	$C_{96}O_4$
C-O-S	$C_{62}O_{22}S_{14}Cl_1$	$C_{51}O_{22}S_{25}Cl_2$	
C-O-Ca	$C_{52}O_{30}Ca_{18}$	$C_{47}O_{30}Ca_{18}$	$C_{82}O_{10}Ca_6$
C-O-Al-Si	$C_{45}O_{30}Al_5Si_{11}Ca_1Fe_4N_{i2}$	$C_{25}O_{44}Al_6Si_{21}K_2$	$C_{50}O_{26}Al_7Si_{15}Fe_1$
C-O-K-Cl		$C_{51}O_{41}K_3Cl_4Ca_1$	

[1] average composition in wt% with accuracy of 1%.

Ni, and Mg, showing the typical irregular morphology of aluminosilicates.

Following fire emission, the morphology and composition of smoke aerosols is changing due to condensation of volatile organic/inorganic species and heterogeneous reactions with gaseous species while smoke is cooling. The changes in the fractions in aged pine smoke are shown Fig. 4. The fraction C-O decreased to 42%, while the fraction C-O-S significantly increased, 7 times, up to 26% due to condensation of sulfur-containing compounds and sulfate formation. A new fraction C-O-K-Cl appeared, with particles of irregular morphology dominated by K and Cl after C and O, and with minor S and Ca content, demonstrating the formation of KCl, K_2SO_4, and $CaCl_2$ salts, (Figs. 1.7–9).

Categorization with Respect to Hygroscopicity

Results obtained from analysis of bulk water uptake, hygroscopic growth, and light scattering of humidified particles are the averaged contribution of different particles that have various morphological, chemical, and therefore hygroscopic properties (Koehler *et al.*, 2009; Petters *et al.*, 2009; Carrico *et al.*, 2010). In BB small-scale studies of Hand *et al.* (2010), smoke aerosols were reported to be internally mixed and composed of inorganic salt species (KCl, K_2SO_4, KNO_3, $(NH_4)_2SO_4$, NH_4Cl), carbon (OC and EC), and soil (Al_2O_3 and CaO). Therefore, the averaged characteristics of smoke hydration properties were obtained such as non-hygroscopic for ponderosa pine or more hygroscopic for sage/rabbit brush burning. The smoke hygroscopic growth was simulated by assuming only inorganic constituents being hygroscopic, when in fact SEM images suggested heterogeneous particles that may be internally or externally mixed (Hand *et al.*, 2010).

Fresh Smoke

To examine the hygroscopicity of each particle fraction produced in the flaming phase of Siberian biomass, we performed water uptake measurements on reference and laboratory-simulated soots. EC soot with no oxygen-containing functionalities or water-soluble organic coatings exhibited extremely hydrophobic character (Popovicheva *et al.*, 2009). Therefore, we consider all particles in the fraction C of fresh pine and debris smoke to be hydrophobic (HPO). Water adsorption by oxygen-containing functionalities following cluster formation and the water film extension over the surface due to the cluster confluence leads to oxidized soot which becomes hydrophilic (HPI) (Popovicheva *et al.*, 2009). Therefore, the O content is used as a measure for categorizing the particles in the fraction C-O of pine and debris smoke as either hydrophobic or hydrophilic.

DFF soot contains only the C-O fraction with low oxygen content up to 7%. Its isotherm is less than the lower boundary of existence of the water film on the soot surface (Fig. 5(a)). Therefore, we accept 7% for O/C as benchmark for definition of hydrophobic particles within the C-O fraction of smoke particles. Analysis of the particle proportion in the C-O fraction shows that in fresh pine and debris smoke 56.5% and 90.5% of total particles, respectively, contain oxygen up to 7% (Fig. 6). This means that these numbers of particles in the C-O fraction can be categorized as hydrophobic.

The isotherm of PBS soot with oxygen content up to 12% approaches the area of the water film existence (Fig. 5(a)). We accept 12% of O/C as critical value for definition of hydrophilic particles of oxidized soot and conclude that about 16% and 4.5% of hydrophilic particles occur within the C-O fraction of fresh pine and debris smoke, respectively. The remaining part of particles with O/C higher than 12% is considered to be hygroscopic (SCOP). Fig. 7 summarizes the statistical breakdown of soot particles in the C-O fraction into HPO, HPI and SCOP percentages following the presented approach. It is noteworthy that more hydrophobic emissions were observed from debris compared to pine fires, probably due to production of less oxidized chemical compounds during combustion. In the small-scale study by Hand *et al.* (2010) the scanning electron microscopy analysis revealed weak and non-hygroscopic particles, quantified by humidification factors, which were dominated by soot and organic constituents. These observations are qualitatively well in accordance with our observations of HPO and HPI particles in the C and C-O fractions.
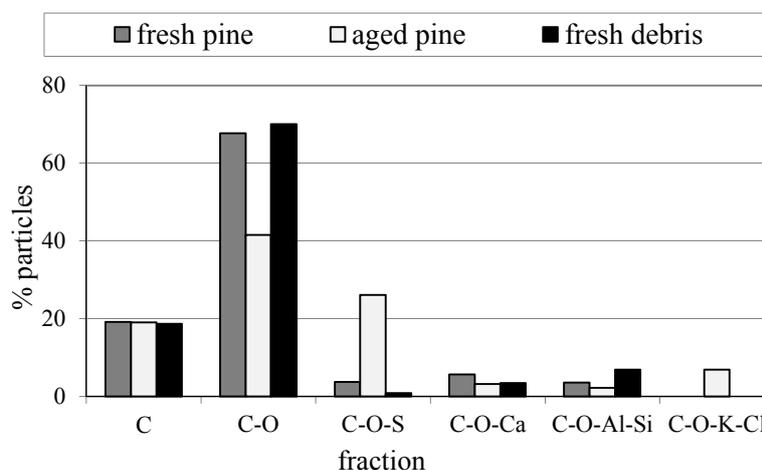

Fig. 4. Percentage of particles (% of total) in C, C-O, C-O-S, C-O-Ca, C-O-Al-Si, and C-O-K-Cl fractions of fresh and aged pine, and fresh debris smoke.
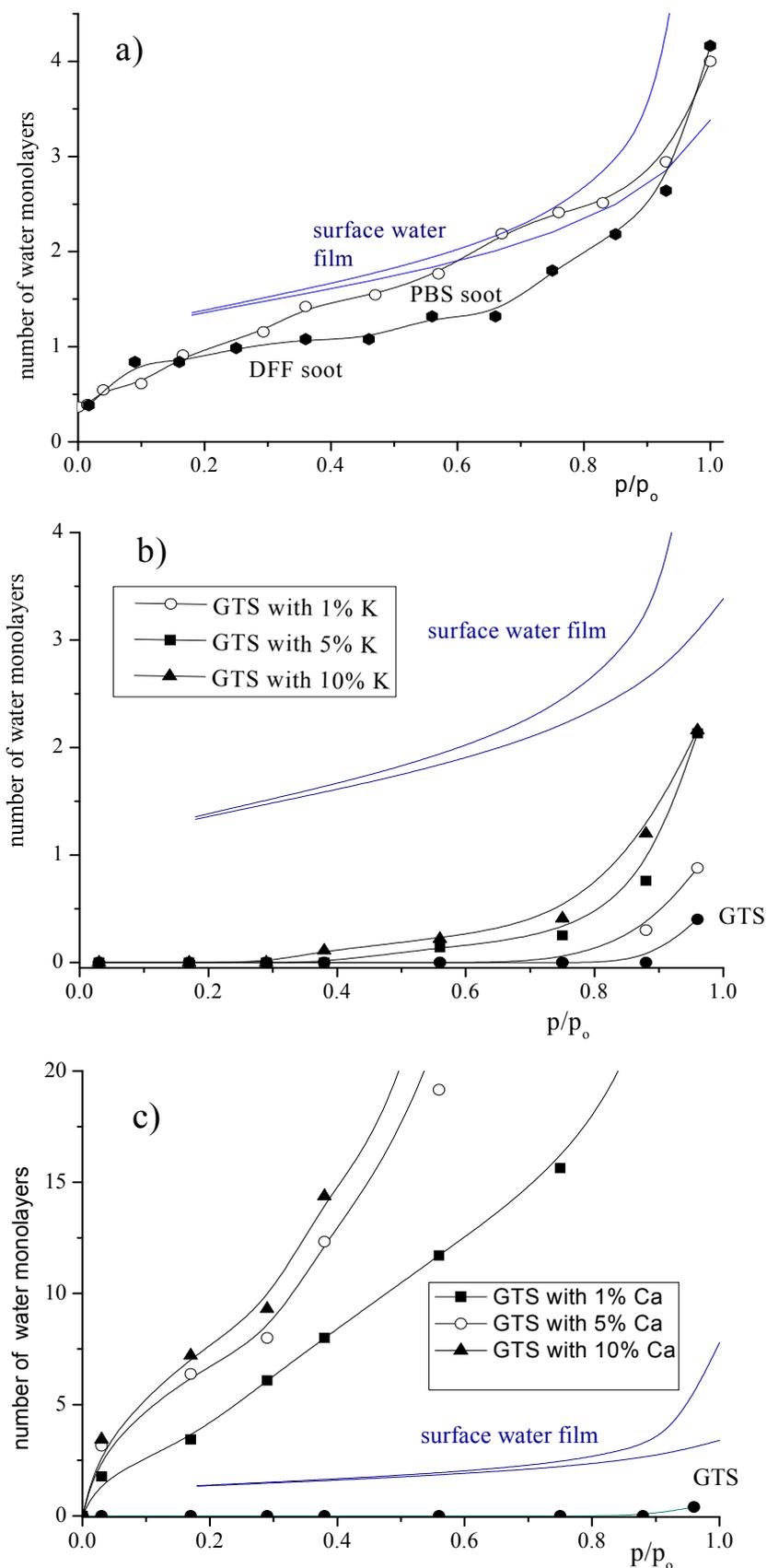
Fig. 5. Isotherms of water absorption a) on DFF and PBS reference soots, b) GTS and GTS with 1% K, 5% K, and 10% K in KCl, and c) GTS with 1% K, 5% K, and 10% K in CaCl$_2$. The area of existence for a water film on the surface is indicated, with low and high boundaries for 20 nm and 250 diameter particles, respectively.
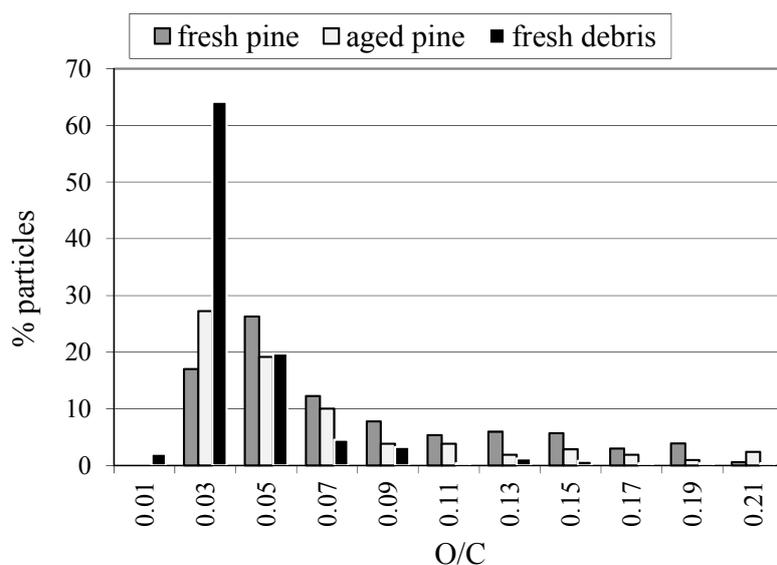
Fig. 6. Percentage of particles (% of total) with various O/C ratios in C-O fraction of fresh and aged pine, and fresh debris smoke.
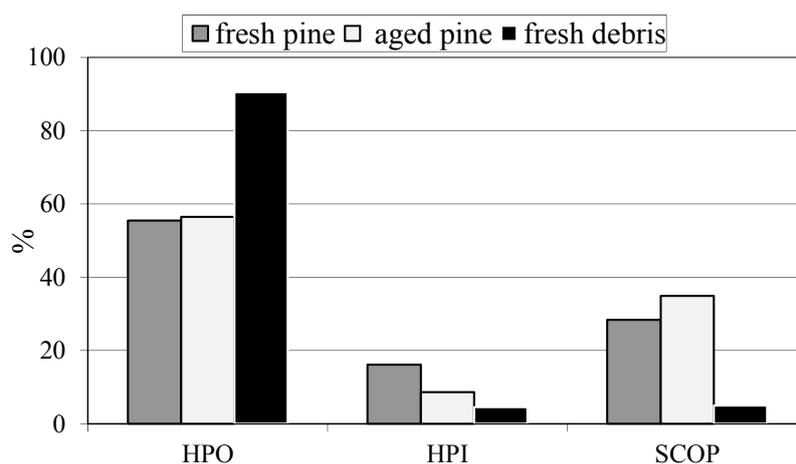

Fig. 7. Proportion of hydrophobic (HPO), hydrophilic (PHI), and hygroscopic (SCOP) particles in C-O fractions of fresh and aged pine, and fresh debris smoke.

The O/C ratio in the C-O-S fraction of fresh pine and debris smoke is found to be significantly higher than in the C-O fraction because of the internal mixing with sulfates. The presence of sulfur in the C-O-S fraction leads to the increase of particle hydrophilicity in comparison with soot containing only oxygen because of the presence of either sulfuric acid condensed on the soot surface or sulfates due to inorganic salt formation. It was found that reference hydrophobic soot with around 3 wt% and 9 wt% of H_2SO_4 changes the ability to absorb water by hydrophilic and hygroscopic particles, respectively (Popovicheva *et al.*, 2011). Since in the C-O-S fraction of pine smoke sulfur is found on average at around 14 wt% (Table 2), we consider all particles in this fraction to be hygroscopic. Carbonaceous particles (soot and organic particles) processed with sulfate species have also been shown to undergo enhancements in particle hygroscopicity (Zhang *et al.*, 2008).

The O/C ratio in the fraction C-O-Ca of fresh pine and debris smoke is found to be significantly higher than in the C-O fraction as well because of the internal mixture with calcium oxides and carbonates. When applying the approach developed above for only carbonaceous particles in the C-O fraction, 8% of total particles should be found to be PHI, while others are SCOP. In the presence of water and CO_2 in the fire emissions CaO and $CaCO_3$ can be transformed to hydroxides $(Ca(OH)_2)$ and bicarbonates $(Ca(HCO_3)_2)$, respectively. Around 0.6% of Ca^{2+} ions were measured in $PM_{2.5}$ in pine smoke (Popovicheva *et al.*, 2015b), demonstrating the presence of calcium salts. In this fraction calcium is found on average with 18 wt% and 6 wt% in fresh pine and debris smoke, respectively (Table 2). Since hydroxides and bicarbonates are water soluble, we relate all particles in the fraction C-O-S to hygroscopic ones.

Fe, Mg-aluminosilicates immersed into carbonaceous matrix comprise the C-O-Al-Si fraction of fresh pine and debris smoke. They are known as hydrophilic materials

(van Oss and Giese, 1995; Tarasevich, 2001). If applying the approach developed for the C-O fraction above only to carbonaceous particles in the C-O-Al-Si fraction, 5% of total particles should be PHI, while others are SCOP, suggesting that aluminosilicates are present in the hygroscopic matrix and increase its ability to take up water.

Previous small-scale BB studies (Petters *et al.*, 2009) showed more and less hygroscopic growth for any particle sizes. Comparisons between growth factor-derived and CCN-derived hygroscopicities were consistent when they were taking into account the composition heterogeneity and assuming externally mixed particles which can act as cloud droplets between 0.2 and 1% supersaturation. They do not require the conversion in the atmosphere to more hygroscopic species before particles can participate in cloud formation processes and undergo wet deposition. Cloud condensation nuclei measurements in the smoke plumes in ambient environments suggested all particles > 100 nm were active at 0.5% water supersaturation, confirming the relatively high hygroscopicity of freshly-emitted particles (Pratt *et al.*, 2011).

Aged Smoke

During aging in the LAC, the smoke constituents were observed to undergo complex transformations. While a number of HBO particles in the C fraction of aged pine smoke remains the same, because the abundance of this fraction was steady (Fig. 4), the proportion of particles with different hydration properties within the C-O was changing. HPI decreased down to 8.6%, SCOP increased up to 35% (Fig. 7), according to the changing OC distribution across particles (Fig. 6), and increasing OC/EC ratio of condensed organic species in cooling smoke found by Popovicheva *et al.* (2015b). Weight percentages of sulfur in condensed sulfates of the C-O-S fraction increased up to 25% (Table 2), undoubtedly leading to high hygroscopicity of all particles in this fraction. In the fraction C-O-Al-Si the weight percent of Al and Si increased up to 16 wt% and 21 wt%, respectively, reflecting the additional release of fly ash during biomass burning and the growth of this fraction's particle hygroscopicity. However, the averaged composition of the C-O-Ca is not changing in aged smoke (Table 2), indicating the impact of soil dust in ambient air used for the chamber filling.

A new fraction C-O-K-Cl of 7% of total particles formed in aged pine smoke (Fig. 4), well in accordance with an increased abundance of K, Cl, and S (Fig. 3). In this fraction 60% of all particles were found in form of KCl, 20% consisted of $CaCl_2$ mixed with low S, and another 20% contained only Cl. This finding confirms the assumption of Liu *et al.* (2000) that potassium organically bound in fluids of vegetation can be evaporated during burning, and further oxidation leads to nucleation and condensation of potassium salts in smoke particles. Elevated concentrations of K^+ ions found in aged smoke in comparison with fresh fire-emitted particles (Popovicheva *et al.*, 2015b) confirm potassium salt formation, well in line with their observations during BB episodes (Engling *et al.*, 2011) and wildfire events (Popovicheva *et al.*, 2014a).

The K/C ratio ≈ 5% found in the fraction C-O-K-Cl was simulated by deposition of aqueous KCl solution of a given concentration on GTS soot. The isotherm of water uptake on GTS soot and on mixtures of GTS with 1, 5, and 10% of K in KCl is shown in Fig. 5(b). No significant increase in hydration properties of hydrophobic GTS matrix is observed due to presence of KCl inclusions. However, a different effect of the inclusion of $CaCl_2$ salt into hydrophobic carbonaceous matrix is found. Isotherms in Fig. 5(c) show high hygroscopicity of mixtures of GTS with 1, 5, and 10% of Ca in $CaCl_2$, significantly exceeding the area of the water film existence. Since the Ca/C ratio in the fraction C-O-K-Cl is found near 1% we conclude that Ca in soluble inorganic salt exerts the largest effect of hygroscopicity between inorganic inclusions.

In BB small-scale studies of Hand *et al.* (2010) hygroscopic particles contained soot chains either internally or externally mixed with inorganic potassium salts. The most hygroscopic smoke particles had the highest inorganic salt to carbon ratios. Carrico *et al.* (2010) reported a similar relationship for measurements of hygroscopicity. Enhancement of hygroscopicity of carbonaceous biomass burning particles mixed internally and externally with inorganic species during the ambient study was also reported by Semeniuk *et al.* (2007). Moreover, the carbonaceous matrix in the fraction C-O-K-Cl of aged pine smoke contains oxygen at the average O/C ratio equal 80%. This extremely oxygen-rich matrix itself provides a much high effect of hygroscopicity than all inorganic inclusions.

CONCLUSIONS

An approach for quantification of BB hygroscopicity at the microscopic level was successfully extended from fossil fuel high-temperature combustion to open flame biomass burning. Fractionation analysis generates a number of particle fractions in Siberian pine and debris smoke produced in small-scale fires in a Large Aerosol Chamber. The fractions of soot particles are observed in fresh smoke alongside fly ash containing inorganic inclusions such as S, Ca, Al, and Si.

To be able to differentiate between smoke particles and discriminate them according to their hydration properties, the morphology and elemental composition data are examined. Water uptake measurements on reference soots are used, and additionally performed for quantification of hygroscopicity of inorganic inclusions in the carbonaceous matrix. It is found that Siberian pine and debris smoke in the flaming phase exhibits a widely heterogeneous mixture of particles with various abilities to take up water: from extremely hydrophobic (of pure elemental carbon particles), through a mixture of hydrophobic, hydrophilic, and hygroscopic carbonaceous particles, according to the oxygen content, to very hygroscopic particles containing inorganic salts.

The relative abundance of each fraction, its categorization and separation of particles inside the fraction provide an estimate for the total abundance of hygroscopic and non-hygroscopic particles. In fresh emissions from flaming fires we obtained 57% and 82% of PHO, 11% and 3% of PHI, and 32% and 15% of SCOP particles in pine and debris smoke,

respectively. In general, smoke produced by small-scale flaming fires of debris from coniferous forest is less hygroscopic than of pine wood fires.

Inorganic species formed during flaming fires of coniferous forest biomass are emitted as part of hygroscopic particles, without the influence of sunlight or atmospheric processing. Similar results were reported by Carrico *et al.* (2010), Petters *et al.* (2009), and Hand *et al.* (2010), utilizing different measurements approaches. However, in Hand *et al.* (2010) only inorganic constituents were considered to be hygroscopic. In our study between carbonaceous particles there is oxidized soot which can be covered by many monolayers of water in a humid atmosphere, demonstrating hygroscopic properties.

During smoke aging in the LAC the condensation of semivolatile organic vapors and inorganic constituents leads to the mixing of soot with unburned organics, sulfates, and mineral fly ash. The increase of the fraction of soot particles internally mixed with sulfates represents an important aging pathway. Together with the newly-formed fraction of potassium and calcium chlorides they enhance the initial level of hygroscopicity in aged pine smoke, resulting in the total SCOP increasing from 32 to 77%. Combining all of the obtained data sets provides new understanding of aerosol hygroscopicity of freshly-emitted and aged smoke in a dark environment, representing near source emissions from open-flame Siberian wildfires in a humid atmosphere at night time. The condensation of sulfates and inorganic salt in aging plumes is expected to increase the hygroscopicity and enable these particles to act more efficiently as CCN at low supersaturation. The findings from this study help to determine the potential impacts of wildfires on cloud-forming potential of smoke aerosols, CCN/IN formation in the atmosphere, and assessing the role of smoke in climate change, specifically related to wildfires in the Northern hemisphere.

REFERENCES

Andreae M.O. and Rosenfeld D. (2008). Aerosol–cloud–precipitation interactions. Part 1. The nature and sources of cloud-active aerosols. *Earth Sci. Rev.* 89: 13–41.

Carrico, C.M., Petters, M.D., Kreidenweis, S.M., Sullivan, A.P., McMeeking, G.R., Levin, E.J.T., Engling, G., Malm, W.C. and Collett Jr, J.L. (2010). Water uptake and chemical composition of fresh biomass smoke. *Atmos. Chem. Phys.* 10: 5165–5178.

Chakrabarty, R.K., Moosmuller, H., Garro, M.A., Arnott, W.P., Walker, J.W., Susott, R.A., Babbitt, R.E., Wold, C.E., Lincoln, E.N. and Hao, W.M. (2006). Emissions from the laboratory combustion of wildland fuels: Particle

morphology and size, *J. Geophys. Res.* 111: D07204, doi: 10.1029/2005JD006659.

Engling, G., Zhang, Y.N., Chan, C.Y., Sang, X.F., Lin, M., Ho, K.F., Li, Y.S., Lin, C.Y. and Lee, J. (2011). Characterization and sources of aerosol particles over the southeastern Tibetan Plateau during the Southeast Asia biomass-burning season. *Tellus Ser. B* 63: 117–128.

Hand, J.L., Day, D.E., McMeeking, G.M., Levin, E.J.T., Carrico, C.M., Kreidenweis, S.M., Malm, W.C., Laskin, A. and Desyaterik, Y. (2010). Measured and modeled humidification factors of fresh smoke particles from biomass burning: role of inorganic constituents. *Atmos. Chem. Phys.* 10: 6179–6194.

Ito, A. and Penner, J. (2005). Historical emissions of carbonaceous aerosols from biomass and fossil fuel burning for the period 1870-2000. *Global Biogeochem. Cycles* 19: GB2028.

Kireeva, E., Popovicheva, O., Persianhtseva, N., Timofeyev, M. and Shonija, N. (2009). Fractionation analysis of transport engine-generated soot particles with respect to hygroscopicity. *J. Atmos. Chem.* 64: 129–147.

Koehler, K., DeMott, P., Kreidenweis, S., Popovicheva, O., Petters, M., Carrico, C., Kireeva, E., Khokhlova, T. and Shonija, N. (2009). Cloud condensation nuclei and ice nucleation activity of hydrophobic and hydrophilic soot particles. *Phys. Chem.* 11: 7906–7920.

Lavoué, D.C., Liousse, C., Cachier, H., Stocks, B.J. and Goldammer, J.G. (2000). Modelling of carbonaceous particles emitted by boreal and temperate wildfires at northern latitudes. *J. Geophys. Res.* 105: 26871–26890.

Li, C., Ma, Z., Chen, J., Wang, X., Ye, X., Wang, L., Yang, X., Kan, H., Donaldson, D.J. and Mellouki, A. (2015) Evolution of biomass burning smoke particles in the dark. *Atmos. Environ.* 120: 244–252.

Mieville, A., Granier, C., Liousse, C., Guillaume, B., Mouillot, F., Lamarque, J.F., Grégoire, J.M. and Pétron, G. (2010). Emissions of gases and particles from biomass burning during the 20th century using satellite data and an historical reconstruction. *Atmos. Environ.* 44: 1469–1477.

Okada, K. and Hitzenberger, R.M. (2001) Mixing properties of individual submicrometer aerosols particles in Vienna. *Atmos. Environ.* 35: 5617–5628.

Paris, J.D., Stohl, A., Nédélec, P., Arshinov, M.Y., Panchenko, M.V., Shmargunov, V.P., Law, K.S., Belan, B.D. and Ciais, P. (2009). Wildfire smoke in the Siberian Arctic in summer: source characterization and plume evolution from airborne measurements. *Atmos. Chem. Phys.* 9: 9315–9327.

Petters, M., Carrico, C., Kreidenweis, S., Prenni, A., DeMott, P., Collett, J. and Moosmuller, H. (2009). Cloud condensation nucleation activity of biomass burning aerosols. *J. Geophys. Res.* 114: D22205, doi: 10.1029/2009JD012353.

Popovicheva, O.B., Persiantseva, N.M., Kuznetsov, B.V., Rakhmanova, T.A., Shonija, N.K., Suzanne, J. and Ferry, D. (2003). Microstructure and water adsorbability of aircraft combustor and kerosene flame soots: Toward an aircraft generated soot laboratory surrogate. *J. Phys.*

Chem. 107: 10046–10054.

Popovicheva, O.B., Persiantseva, N., Shonija, N., DeMott, P., Koehler, K., Petters, M., Kreidenweis, S., Tishkova, V., Demirdjian, B. and Suzanne, J. (2008a). Water interaction with hydrophobic and hydrophilic soot particles. *Phys. Chem.* 10: 2332–2344.

Popovicheva, O., Persiantseva, N., Tishkova, V., Shonija, N. and Zubareva, N. (2008b) Quantification of water uptake by soot particles. *Environ. Res. Lett.* 3: 025009, doi: 10.1088/1748-9326/3/2/025009.

Popovicheva, O.B., Kireeva, E.D., Shonija, N.K. and Khokhlova, T.D. (2009). Water interaction with laboratory-simulated fossil fuel combustion particles. *J. Phys. Chem. A* 113: 10503–10511.

Popovicheva, O.B., Persiantseva, N.M., Kireeva, E.D., Khokhlova, T.D. and Shonija, N.K. (2011). Quantification of the hygroscopic effect of soot aging in the atmosphere: Laboratory simulations. *J. Phys. Chem.* 115: 298–306.

Popovicheva, O., Kistler, M., Kireeva, E., Persiantseva, N., Timofeev, M., Kopeikin, V. and Kasper-Giebl, A. (2014a). Physicochemical characterization of smoke aerosol during large-scale wildfires: Extreme event of August 2010 in Moscow. *Atmos. Environ.* 96: 405–414.

Popovicheva, O.B., Kireeva, E.D., Steiner, S., Rothen-Rutishauser, B., Persiantseva, N.M., Timofeev, M.A., Shonija, N.K., Comte, P. and Czerwinski, J. (2014b). Microstructure and chemical composition of diesel and biodiesel particle exhaust. *Aerosol Air Qual. Res.* 14: 1392–1401.

Popovicheva, O., Engling, G., Lin, K.T., Persiantseva, N., Timofeev, M., Kireeva, E., Volk, P., Hubert, A. and Wachtmeister, G. (2015a). Diesel/biofuel exhaust particles from modern internal combustion engines: microstructure, composition, and hygroscopicity. *Fuel* 157: 232–239.

Popovicheva, O.B., Kozlov, V.S., Engling, G., Diapouli, E., Persiantseva, N.M., Timofeev, M.A., Fan, T.S., Saraga, D. and Eleftheriadis, K. (2015b). Small-scale study of Siberian biomass burning: I. Smoke microstructure. *Aerosol Air Qual. Res.* 14: 1392–1401.

Pratt, K.A., Murphy, S.M., Subramanian, R., DeMott, P.J., Kok, G.L., Campos, T., Rogers, D.C., Prenni, A.J., Heymsfield, A.J., Seinfeld, J.H. and Prather, K.A. (2011). Flight-based chemical characterization of biomass burning aerosols within two prescribed burn smoke plumes. *Atmos. Chem. Phys.* 11: 12549–12565.

Rakhimov, R.F., Kozlov, V.S. and Shmargunov, V.P. (2012). On time dynamics of the complex refractive index and particle microstructure according to data of spectronephelometer measurements in mixed composition smokes. *Atmos. Oceanic Opt.* 25: 51–61.

Rakhimov, R.F., Kozlov, V.S., Panchenko, M.V., Tumakov, A.G. and Shmargunov, V.P. (2014). Properties of atmospheric aerosol in smoke plumes from forest fires according to spectronephelometer measurements. *Atmos. Oceanic Opt.* 27: 275–282.

Reid, J., Koppmann, R., Eck, T. and Eleuterio, D.P. (2005). A review of biomass burning emissions part II. Intensive physical properties of biomass burning particles. *Atmos. Chem. Phys.* 5: 799–825.

Semeniuk, T.A., Wise, M.E., Martin, S.T., Russell, L.M. and Buseck, P.R. (2007). Hygroscopic behavior of aerosol particles from biomass fires using environmental transmission electron microscopy. *J. Atmos. Chem. 56*: 259–273.

Tarasevich, Y.I. (2001). Interaction of water and other polar substances with various sorbents according to calorimetric and chromatographic data. *Theor. Exp. Chem.* 37: 199–215.

Treffeisen, R., Tunved, P., Strom, J., Herber, A., Bareiss, J., Helbig, A., Stone, R.S., Hoyningen-Huene, W., Krejci, R., Stohl, A. and Neuber, R. (2007). Arctic smoke – aerosol characteristics during a record smoke event in the European Arctic and its radiative impact. *Atmos. Chem. Phys.* 7: 3035–3053.

van der Werf, G.R., Randerson, J.T., Giglio, L., Collatz, G.J., Mu, M., Kasibhatla, P.S., Morton, D.C., DeFries, R.S., Jin, Y. and van Leeuwen, T.T. (2010). Global fire emissions and the contribution of deforestation, savanna, forest, agricultural, and peat fires (1997–2009). *Atmos. Chem. Phys.* 10: 11707–11735.

van Oss, C.J. and Giese, R.F. (1995). The hydrophilicity and hydrophobicity of clay minerals. *Clays Clay Miner.* 43: 474–477.

Warneke, C., Froyd, K.D., Brioude, J., Bahreini, R., Brock, C.A., Cozic, J., De Gouw, J., Fahey, D.W., Ferrare, R., Holloway, J.S., Middlebrook, A., Miller, L., Montzka, S., Schwarz, J.P., Sodemann, H. and Spackman, J.R. (2010). An important contribution to springtime Arctic aerosol from biomass burning in Russia. *Geophys. Res. Lett.* 37: L01801, doi: 10.1029/2009GL041816.

Yun, Y., Penner, J.E. and Popovicheva, O. (2013). The effects of hygroscopicity on ice nucleation of fossil fuel combustion aerosols in mixed-phase clouds. *Atmos. Chem. Phys.* 13: 4339–4348.

Zhang, R., Khalizov, A.F., Pagels, J., Zhang, D., Xue, H. and Mc-Murry, P.H. (2008). Variability in morphology, hygroscopicity, and optical properties of soot aerosols during atmospheric processing. *Proc. Natl. Acad. Sci. U.S.A.* 105: 10291–10296.